Inorganic Chemistry Communications 144 (2022) 109930

Contents lists available at ScienceDirect

Inorganic Chemistry Communications

journal homepage: www.elsevier.com/locate/inoche

Short communication

Biogenic synthesis of nickel oxide nanoparticles using *Averrhoa bilimbi* and investigation of its antibacterial, antidiabetic and cytotoxic properties

V. Haritha [a], S. Gowri [b], B. Janarthanan [a], Md. Faiyazuddin [c,d,*], C. Karthikeyan [e], S. Sharmila [a,*]

[a] Energy and Nano Research Laboratory, Department of Physics, Karpagam Academy of Higher Education, Coimbatore, Tamil Nadu, India
[b] PG & Research Department of Physics, Cauvery College for Women, Tiruchirapalli, Tamil Nadu, India
[c] School of Pharmacy, Al – Karim University, Katihar, Bihar, India
[d] Nano Drug Delivery®, Raleigh-Durham, NC 27705, USA
[e] KIRND Institute of Research and Development PVT LTD, Tiruchirappalli, Tamil Nadu 620 020, India

ARTICLE INFO

Keywords:
Nickel oxide nanoparticles
Averrhoa bilimbi
Antibacterial
Antidiabetic
Anticancer

ABSTRACT

Numerous methods have been implemented to prepare nickel oxide nanoparticles many of which involve harmful chemicals that can be avoided by using plant or fruit extracts. In the present work, we have prepared nickel oxide nanoparticles using extract of *Averrhoa bilimbi* fruit. The bioactive compounds like tannins, flavonoids, and phenols present in the fruits act as a reducing and capping agent to convert nickel nitrate to nickel oxide nanoparticles. The prepared nanoparticles are subjected to structural, optical, and morphological analysis by Powder X-ray Diffraction pattern (P-XRD), Fourier Transform-Infrared Spectroscopy (FTIR), UV–visible analysis (UV–vis), Scanning Electron Microscopic technique (SEM), and EDAX analysis. The magnetic property of the prepared nanoparticles is examined by Vibrating Sample Magnetometer (VSM). Nickel Oxide nanoparticles exhibit potent antibacterial activity against *E.coli* and *S.auerus* with a higher region of zone of inhibition at 150 μgmL^{-1}. The antidiabetic effect of the prepared sample is investigated and found to exhibit their inhibitory effect on α-amylase enzyme with IC_{50} value 311.26 μgmL^{-1}($p < 0.005$). Finally, the cytotoxic effects of nickel oxide nanoparticles are studied in cultured human colorectal cancer cells (HCT-116), which have exhibited significant anticancer activity with 55 μgmL^{-1} at 50 % inhibition concentration (IC_{50}). From the results, nickel oxide nanoparticles may offer a safe potential for diabetes and cancer management and can be applied to different medical and industrial applications.

1. Introduction

The most frequent Healthcare Associated Infections (HAIs) are caused by gram-positive and gram-negative bacteria, which can lead to major problems such as renal disease, dysentery, and wound infections, among other things. Bacteria can also cause severe life-threatening complications. Similarly, 'Diabetics' and 'Cancer' are the two more non-communicable diseases that endanger life of humans. According to the World Health Organization (WHO), 10 million people died from cancer in 2020, accounting for 10% of all fatalities. Cancer is treatable if detected in early stage. Chemotherapy, radiation and surgery can be used to treat it have side effects and are more expensive. As a result, researchers around the world are working on their way in designing new tools or advanced inexpensive techniques and multifunctional therapetic drugs to save human lives with negligible side effects. Nanoparticle-based drug administration is more efficient than traditional drug delivery because of its biocompatibility, better stability, and permeability, as well as precise in targeting bacterial infections and cancer cells.

Three mechanism involved in drug delivery resistance such as over expression of drug efflux tranporters, defective apoptotic pathways and hypoxic environement. Due to extensive and intriguing thermal, electrical, optical, magnetic, and medicinal capabilities not exhibited by bulk counterparts, nanoparticles focused on these mechanisms to increase its performance and be the solution to the above-mentioned problem [1–3]. However, these properties depend on the size, structure, morphology and mechanisms of the particles synthesized. When using chemical processes to make nanoparticles, notable challenges include health and environmental concerns. Furthermore, it necessitates expensive specialised equipments, strict protocol, and the production of

* Corresponding authors.
E-mail addresses: md.faiyazuddin@gmail.com (Md. Faiyazuddin), sharmila.s@kahedu.edu.in (S. Sharmila).

https://doi.org/10.1016/j.inoche.2022.109930
Received 1 June 2022; Received in revised form 12 August 2022; Accepted 24 August 2022
Available online 28 August 2022

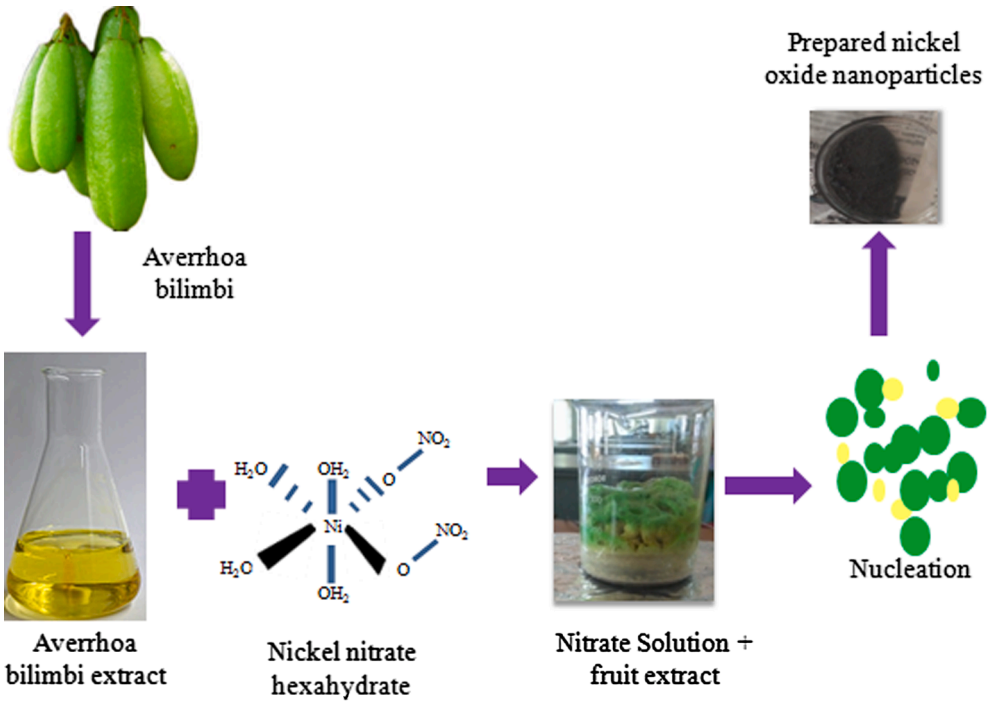

Fig. 1. Synthesis of NiO nanoparticles.

harmful gases during the reaction. Meanwhile, using fungi, yeast, different parts of plants or fruits extract will overcome all the aforementioned issues and the presence of polyphenols, flavonoids, tannins, and other enzymes which varies for plants will act as a reducing and capping agent to prepare nanoparticles without harming nature and humans [4–5].

Averrho abilimbi a multipurpose, long-lived tropical plant belongs to the family '*Oxalidaceae*' commonly known as "Bilimbi" or "cucumber tree". Bilimbi is a nutrient-dense, starchy fruit that grows on the trunks of tall trees and is related to starfruit, which is widely grown in Asian countries. The fruit is high in Vitamin C, and it also contains fibers, protein, anthocyanin, tannins, and minerals. Fever, rectum inflammation, diabetes, rheumatism, whooping cough, stomach ache, ulcer, and other conditions are treated with *Averrhoa bilimbi*. *A. bilimbi* has antidiabetic, anti-microbial, anti-inflammatory, cytotoxic and antioxidant activity. Ascorbic acid, the water-soluble antioxidant compound present in the fruit may acts as a reducing agent and neutralizes Reactive Oxygen Species (ROS) leads to form radical and an electron [6]. Maya S Nair *et al.*, reveal the anticancer activity of *A. bilimbi* leaf and fruit extract on MCF-7 human breast cancer and concluded fruit extract showed good activity than leaf extract [7]. Surya B Kurup and S Mini [8] reported that *Averrhoa bilimbi* fruit showed potential improvement in controlling the level of glucose in the blood, which was further confirmed by testing with five groups of rats.

Among various transition metal oxides (TiO_2, ZnO, CuO, V_2O_5, ZrO), a cubic structured p-type semiconductor nickel oxide (NiO) has attracted massive attention due to its high chemical stability, wide bandgap (3.6 – 4.0 eV), large surface area, high catalytic activity and extends its applications towards wastewater treatment, gas sensors, energy storage devices, antiferromagnetic layer (Neel temperature), photocatalytic degradation of organic dyes, and biomedical applications such as anbacterial agent, cancer diagnosis and therapy and so on [3,9]. Furthermore, due to the generation of Reactive Oxygen Species (ROS), reduction in the size of particles and phytochemicals like alkaloids, flavonoids, tannin and saponins present in the plant extract are reponsible for cell damage. The production of ROS can be affected by different parameters mainly over disturbance in intracellular metabolic activities and irradiance under ultrviolet light [10–11].

Number of reducing and capping agents have been employed by researchers to analyze and investigate the antimicrobial properties of nickel oxide nanoparticles which includes the usage of Arabic gum [12], *Spirostachys Africana* bark [13], *Berberis balochistanica* stem [14], *Solanum trilobatum* [15], *Rhamnus triquetra* [16], *Phoenix dactylifera* [17], ginger and garlic [18], neem [19], Monsonia burkeana [20], *Aegle marmelos* [21], *Allium cepa* [22], *Nephelium lappaceum* [23], *Rhamnus virgata* [24], *Okra plant* [25], *Moringa oleifera* [26], *Tamarix serotina* [27], *Azadirachta indica* and *Psidium guajava* [28], *Ageratum conyzoides* [29], etc. The research intends of the present work is to synthesize nickel oxide nanoparticles using *A. bilimbi* as the reducing and capping agent and to analyze the structure, morphology, optical and microbial properties.

2. Methodology

Averrhoa bilimbi fruits were collected from the local agriculture field of Kerala, India. The collected fruits were washed thrice with running water and with distilled water to remove the dust particles present on the surface. The skin of the fruit was peeled off and the flesh was collected and added to 120 mL of distilled water. The resultant mixture was heated at 60–70 °C and filtered using Whatman No. 1 filter paper and kept separately. 0.5 M of nickel nitrate was added to 100 mL of distilled water and stirred well until it dissolved completely. Later, the solution was mixed with fruit extract (1:1 ratio) drop by drop under constant stirring in the magnetic stirrer. The mixer was stirred well for 2 h under 60 °C and a slight color change was observed in the solution. The color change is caused due to the reaction between the bioactive compounds present in the fruit extract (which acts as a reducing agent) and nickel nitrate solution. When color change occurs, the mixture should be transferred to a hot plate to convert the solution into powder. The resultant powder is calcined in a muffle furnace under 600 °C for 4 hrs and utilized for further analysis. Fig. 1 exhibits the flowchart of the nanoparticle preparation.

2.1. Characterization

The crystalline nature and purity of the prepared nickel oxide can be

verified by Powder X-ray diffraction pattern (XRD) using X'Pert PRO diffractometer equipped with CuKα radiation (λ = 0.1540 nm) with a step size of 0.0500° in the range of 10 to 80°. The nature of the chemical bond and the existed functional groups present in the prepared samples are analyzed using Fourier Transform-Infrared Spectrum. The optical properties of the prepared nanoparticles were examined via Shimadzu-2450 UV–vis Spectrometer. Perkin Elmer-LS 45 spectrometer used to determine the PL spectrum of the prepared nanomaterial. The particle size and its distribution have been analyzed by NanoPlus Dynamic Light Scattering (DLS). The shape, size, and surface morphology of the nanoparticles formed were examined by Scanning Electron Microscopy (ZEISS) and the elemental composition by EDAX spectrum. Vibrating Sample Magnetometer (Cryogenic) was used to examine the nickel oxide nanoparticles' magnetic characteristics at room temperature with the magnetic field of 2kOe.

2.2. Antibacterial assay

Gram-negative bacteria, Escherichia coli (MTCC 732) and Gram-positive bacteria, Staphylococcus aureus (MTCC 3160), were used to investigate the antibacterial activity of the produced NPs. The antibacterial activity of NiO NPs was investigated using the disc diffusion method. 30 mL of nutritional agar medium was used to make the petri plates. To obtain the bacteria's strain, it was dispersed across nutrient agar. In order to investigate the bacterial strain, the sterile filter paper containing samples of 50 L (50μgmL^{-1}), 100 L (100μgmL^{-1}), and 150 L (150 μg mL^{-1}) was distributed on the surface of the infected agar plate and incubated for 24 h at 37 °C (±2). Chloramphenicol was used as a reference. The assay was carried out three times. In millimetres, the inhibitory zone that grew around the disc was measured.

2.3. α-Amylase enzyme assay (AAEA)

To determine the α-Amylase activity, predominantly, the pancreatic α-amylase (class, α-1,4-gluconohydrolases) is considered as one of the key enzymes for diabetes management. Naturally occurring α-amylase enzyme inhibitors from ethnobotanicals have proven themselves as very effective in managing postprandial blood glucose levels [30]. To experiment, 1 mL of buffer (phosphate-buffered saline) was taken in a glass tube and mixed with 0.5 mL sample aliquots of varying concentrations (100, 200, 300, 400, and 500 μg mL^{-1}) or with the standard solution. To the reacting mixture, 200 μL of 0.5 mg ml^{-1}of α-amylase was added and followed by 200 μL of5 mg mL^{-1} starch solution (0.1 % w/v). The mixture was left to react at 25 °C for 10 min. By drop wise addition of 400 μL of normal saline (dextrose normal saline) followed by heating (100 °C, 5 min) and cooling, the reaction was finally stopped. Starch with amylase and without α –amylase is considered as control. The reaction without *Averrhoa bilimbi* unripe fruit extract was used as a control and Metformin HCl was used as a standard. The enzyme activity was recorded as per the formula given below:

$$\text{Inhibition of } \alpha-\text{Amylase activity } (\%) = (\text{Sample})_{\text{Abs}} - (\text{Control})_{\text{Abs}}/(\text{Sample})_{\text{Abs}} \times 100$$

2.4. MTT cytotoxic assay

The cytotoxic activities against HCT116 cancer cell lines were estimated using the MTT assay (3-[4,5-dimethyl-2- thiazolyl)-2,5-diphenyl-2H-tetrazolium bromide), which was based on the reduction of the tetrazolium salt by mitochondrial dehydrogenase in viable cells [30]. Cell culture of HCT116 (human colorectal carcinoma) cell lines were maintained in Dulbecco's Modified Eagle Medium (DMEM) which was supplemented with 10 % heat-inactivated fetal bovine serum (FBS), and 100 U/ml penicillin. In brief, experimental cells were seeded in a 96-well sterile microplate at a density of 1 × 10^4 cells/well and incubated (37 °C with humidified 5 % CO_2 atmosphere) with a series of

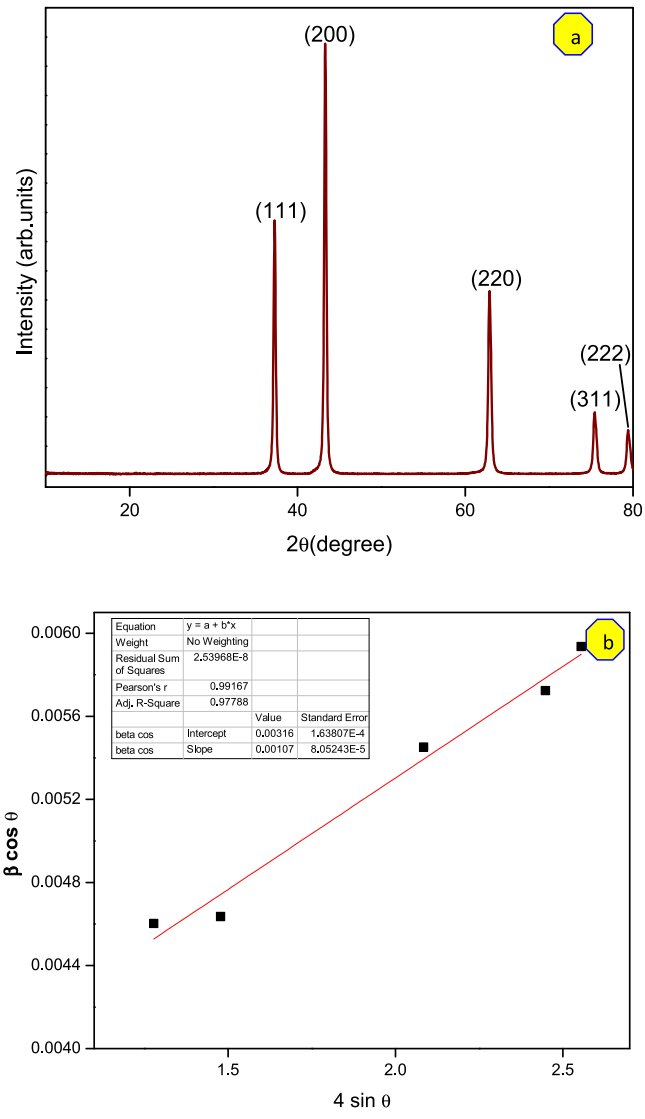

Fig. 2. (a) XRD pattern of NiO (b) W-H plot of NiO nanoparticles.

different concentrations of each trial formulation or cisplatin (positive control) in DMSO for 48 h in a serum-free medium before the MTT assay. After incubation, the culture media was cautiously removed without disturbing the crystal formed, and 40 μL aliquot of MTT was added to each well and then again incubated for 4 hrs. A purple formazan dye crystals were solubilized by the addition of 200 μL of DMSO in a gyratory shaker. The absorbance was measured at 570 nm using a multi-mode microplate reader. For the result analysis, the relative cell viability was expressed as the mean percentage of viable cells compared to the untreated control cells.

2.5. Statistical analysis

Statistical analysis was performed by one-way analysis of variance (ANOVA) followed by Duncan's post hoc test of significance using SPSS (version 16.0).

3. Result and discussion

Fig. 2a exhibits the typical XRD pattern of the nickel oxide powder. All the diffracted peaks show a sharp well defined crystalline nature with a face-centered cubic structure without any impurity. The obtained peak attributes to Fmm space group and matches with JCPDS card no.

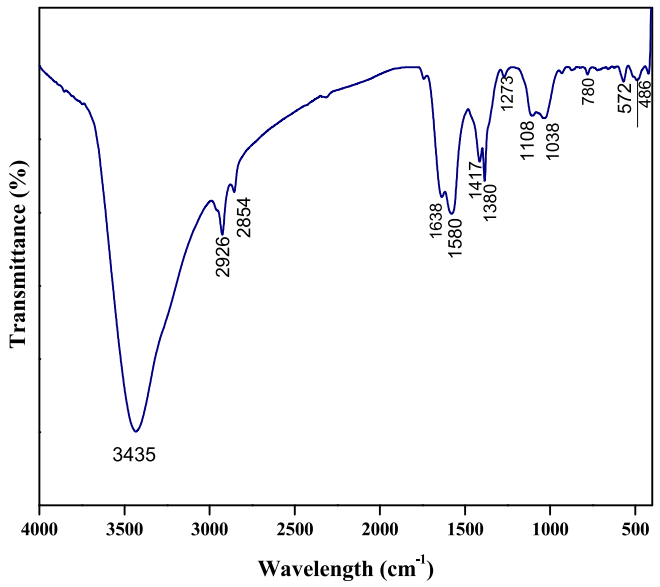

Fig. 3. FT-IR spectrum of NiO nanoparticles.

04–0835 [22]. The 2θ values are observed at 37.2°, 43.3°, 62.9°, 75.4° and 79.4° corresponds to (1 1 1), (2 0 0), (2 2 0), (3 1 1), and (2 2 2) planes respectively. For cubic structured material, eq. (1) can be utilized to calculate the lattice paprameter.

$$1/d^2 = (h^2 + k^2 + l^2)/a^2 \quad (1)$$

where h, k, l represents the miller indices of corresponding angle, a indicates the lattice parameter and d represents inter-planar spacing. The lattice parameter and cell volume of the prepared nickel oxide are calculated as 4.17 Å and 72.7 $Å^3$ matched with earlier reports [22]. The broadening of Bragg's peak at bases also indicates the formation of small-sized nanoparticles [31]. The average crystallite size (28 nm) was estimated using the Debye- Scherrer formula which is lesser as examined by V Helan et al., at three different temperatures and may also result in good antibacterial results [19]. Williamson-Hall analysis was carried by plot between 4 sinθ and β cosθ as shown in Fig. 2b. Using the linear fitting method, the slope and intercept were calculated and the material exhibits a positive slope indicating tensile strain [32–33].

FT-IR is an interesting tool to study the molecules/ compound involved in the chemical reaction. In the synthesis of nanoparticles via the green route, FTIR helps to identify the bioactive compounds involved in the reaction and act as a reducing or capping agent. Fig. 3 exhibits the FT-IR spectrum of prepared NiO nanoparticles. The strong

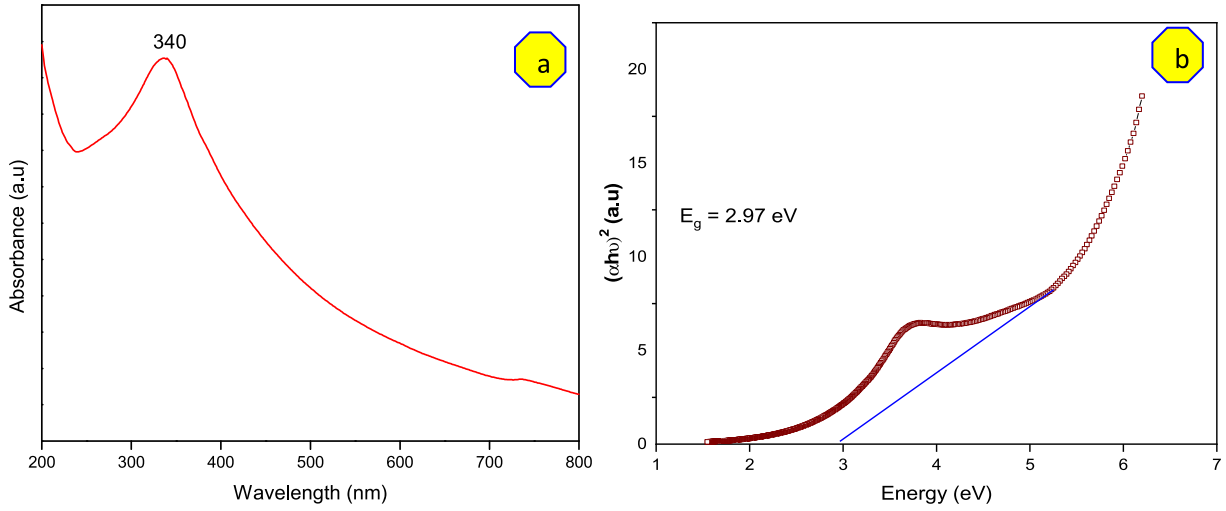

Fig. 4. (a) UV–vis spectrum (b) Bandgap of NiO nanoparticles.

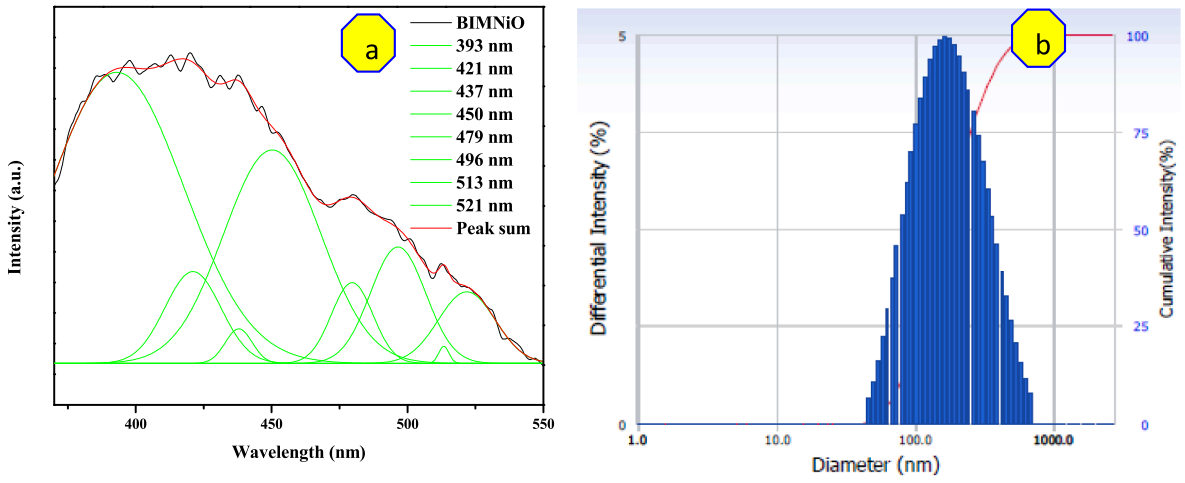

Fig. 5. (a) PL emission (wavelength: 350–550 nm) and (b) DLS spectra of NiO nanoparticles.

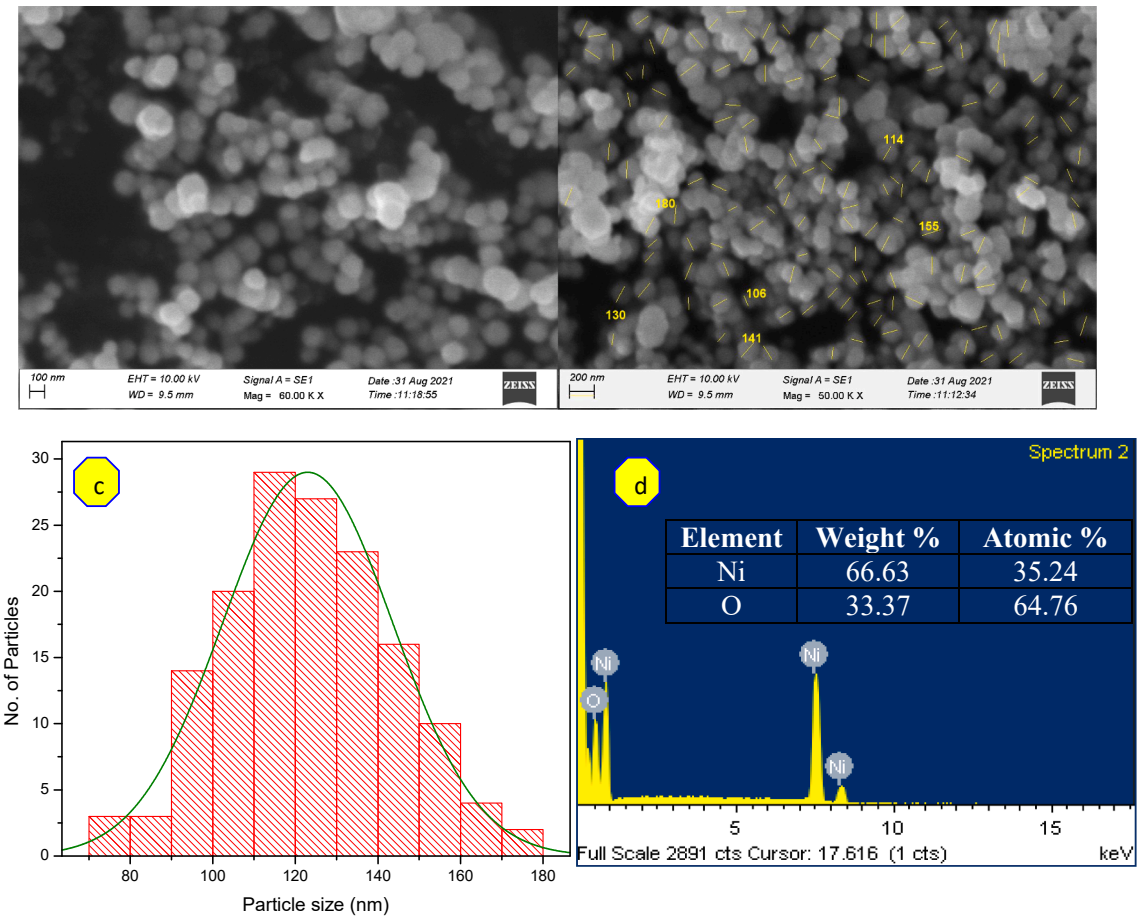

Fig. 6. (a-b) SEM images of NiO nanoparticles (c) Histogram of particle size **(d) EDX analysis.**

broad peak observed at 3435 cm^{-1} attributed to the stretching vibrations of hydroxyl groups of phenols and carboxylic acids. The characteristic peak at 2926 cm^{-1} tends to C—H group. The stretching tertiary vibration of C═O notified at 1638 cm^{-1}. The characteristic peak at 1580, 1417 and 1273 cm^{-1} attributes to stretching vibrations of C═C, —C—O of aromatic groups respectively. The weak aromatic amine group of C—N and C—OH of primary alcohol present in fruit extract observed at 1108 and 1038 cm^{-1}. Metal-Oxygen vibrational peak observed from 780 to 480 cm^{-1} indicates the formation of nanoparticles due to the presence of bioactive compounds such as amines and alcohols present in the fruit extracts which convert nitrates into oxides [34].

Fig. 4a shows the UV–vis spectrum of NiO nanoparticles in the range of 200 to 800 nm. The maximum absorption peak is notified at 340 nm which confirms the formation of nanoparticles which is in agreement with earlier reports [35]. The transit of electrons from the valence band to the conduction band of NiO (O(2p)) to Ni(3d) is linked to a significant absorbance peak [36]. Due to the outcome of ligand to metal charge transfer an absorption peak may be observed. The bandgap of NiO nanoparticles can be calculated using the Tauc plot equation: $(\mu h\upsilon)^n = A(h\upsilon - E_g)$, where $\mu h\upsilon$, E_g, and n take its conventional meaning. The energy bandgap of the material is calculated as 2.97 eV when the sample is calcined at 600 °C and comparable with an earlier report [36] and shown in Fig. 4 (b).

As shown in Fig. 5 (a), the PL spectrum of NiO NPs was stimulated using 325 nm wavelength. For the NiO NPs, the PL emission peaks were found at 393 nm, 421 nm, 437 nm, 450 nm, 479 nm, 496 nm, 513 nm, and 521 nm. During the NBE transition, excitonic recombination of electrons in the conduction band (CB) and holes in the valence band (VB) causes UV emission peaks at 393 nm [37]. The energy transfer of trapped electrons at Ni interstitial (Ni_i) to the valence band corresponds

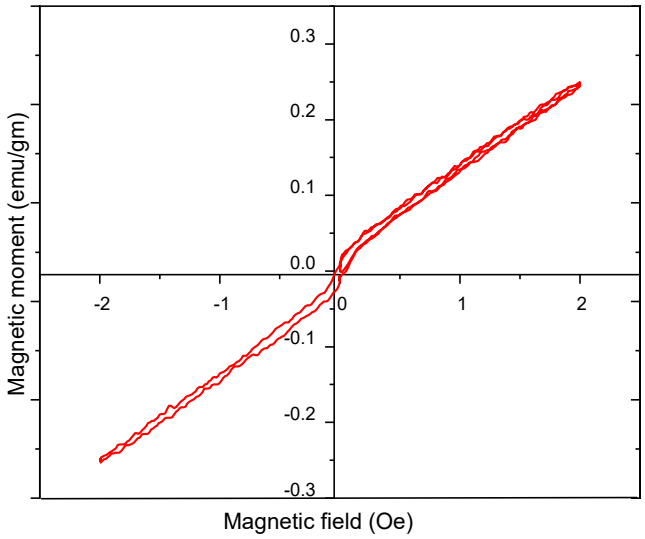

Fig. 7. M-H curve of NiO nanoparticles.

to the violet emission peaks at 421 nm [38]. The radiative recombination of electrons from the doubly ionized Ni vacancy (V_{Ni}^{2-}) to the hole in the VB is represented by blue emission peaks at 437 nm, 450 nm, 479 nm, and 496 nm, respectively [39]. They say the green emission peak seen at 513 nm and 521 nm is caused by surface defects that formed inside the NiO matrix. These defects include interstitial oxygen trapping and Ni vacancies created when the charge is transferred between Ni^{2+}

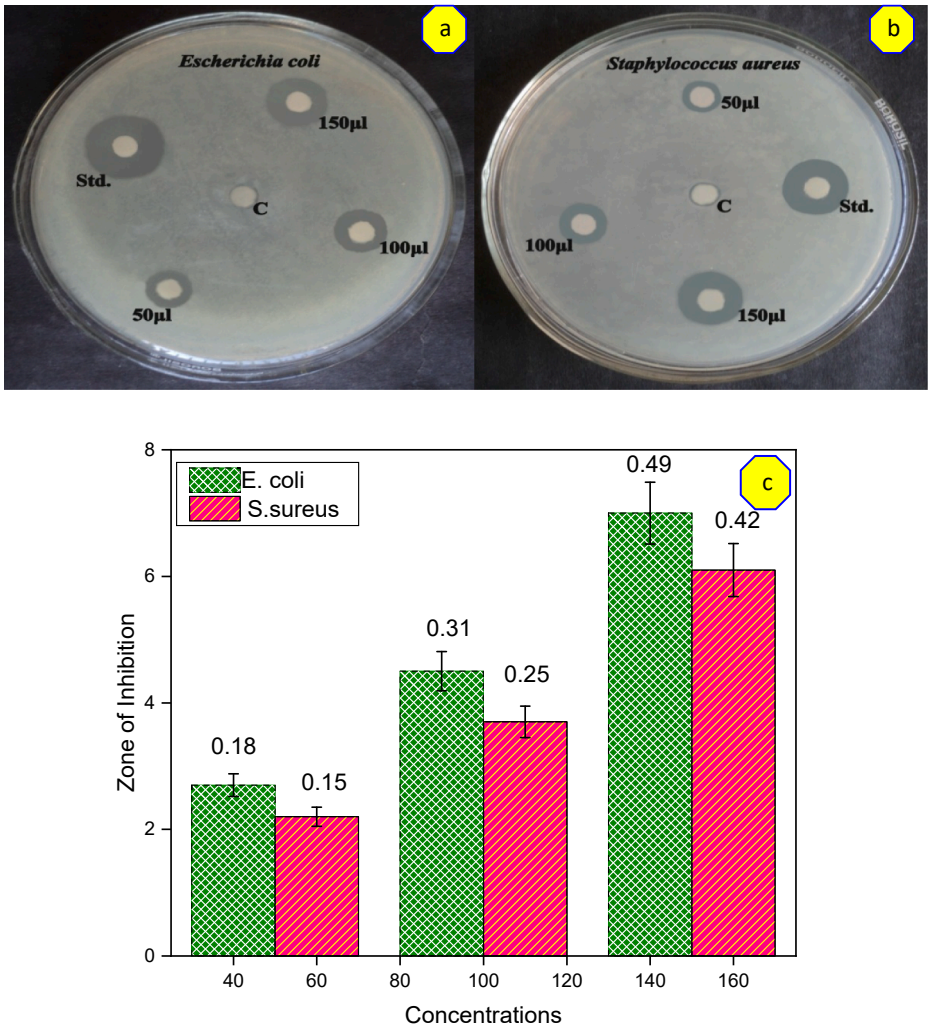

Fig. 8. Antibacterial property of NiO NPs against (a) *E. coli* and (b) *S.aureus* and (c) Zone of inhibition region.

and Ni^{3+} [39]. The Dynamic Light Scattering (DLS) technique investigated the particle size distribution in an aqueous solution. According to the DLS study results, the average size distribution by percentage for NiO NPs was observed at 170 nm (Fig. 5b).

The morphology of the *bilimbi* assisted nickel oxide nanoparticles is examined by using Scanning Electron Microscope. Fig. 6 (a-b) shows the morphology of the nanoparticles. The images predict the formation of spherical-shaped particles with uniform size distribution without any agglomeration. Fig. 6c indicates the particle size histogram and maximum number of particles are observed in the range of 110 to 120 nm. Fig. 6d implicit the EDX analysis, which consists of 66.63 % of Ni and 33.37 % of O elements only. It strongly infers that the prepared sample consists solely of Ni and O without any impurity and supports the results obtained from XRD pattern.

Table 1
Zone of inhibition of NiO NPs against bacterial strain.

Bacterial strain	Zone of inhibition (mm)	Extract	Reference
S. aureus	10	Okra plant	[19]
E. coli	Not appearing		
P. aeruginosa	Not appearing		
S. aureus	5	*Gymnema*	[35]
E. coli	3	*sylvestere*	
S. aureus	6.1 @ 150 µL	*Averrhoa bilimbi*	Present work
E. coli	7 @ 150 µL		

The M-H curve of the produced NiO nanoparticles at room temperature is shown in Fig. 7. When NiO particles are sized in the nano range, the magnetic behaviour of the material exhibits aberrant behavior, which may be caused by finite size, surface effects, anisotropic nature, or spin rate [40,41]. The weak ferromagnetic nature of the material at room temperature was depicted from the plot. The possibility of asperomagnetism or spin-glass behavior of NiO NPs is identified by the absence of a magnetization curve or saturation level due to reduction in size of the particles obtained [32]. Additionally, the superparamagnetism interaction is visible at ambient temperature without coercivity or retentivity [12,41,42], which is also necessity for better biological applications.

The antibacterial analysis of *A.bilimbi* assisted NiO NPs was studied via disc diffusion method by testing the NPs against *E.coli* and *S.aureus* (Fig. 8). Both the plates do not exhibit any zone of inhibition for control, in the meanwhile, the zone of inhibition observed against *E.coli* and *S. aureus* infers that the prepared nanoparticles have good antibacterial properties. The diameter of the inhibited zone ranges from 2.70 mm to 7.00 mm and 2.20 mm to 6.10 mm for *E.coli* and *S.aureus* respectively. The zone of inhibition increases with an increase in concentration and the higher region is observed at 150 µg mL^{-1}. Compared to the gram-positive bacteria, the prepared nanoparticles have a good antibacterial properties to penetrate the complex cell membrane of gram-negative bacteria for all three concentrations as shown in Fig. 8 (a-c). In general, changes in the particle size, concentration of the precursors, pH of the solution prepared and surface defects present on the synthesized

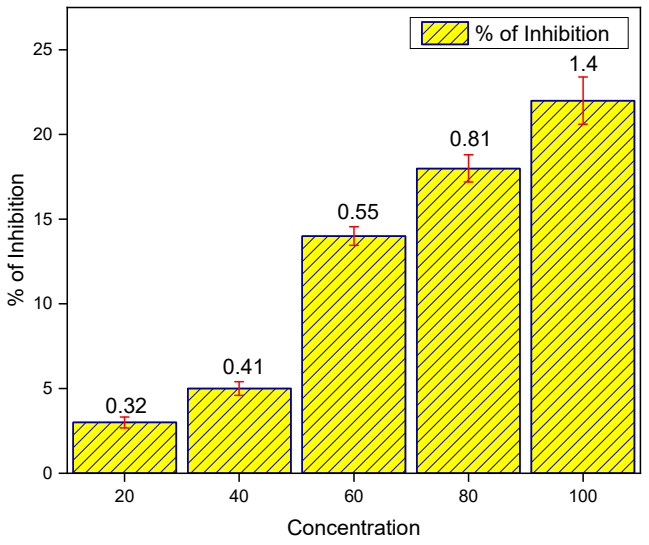

Fig. 9. Inhibitory potential of NiO NPs on α-amylase enzyme activity.

Table 2
Comparative study of % of inhibition.

Concentration (μg/ml)	% Inhibition –NiO NPs	
	Present work	[44]
20	3	3.35
40	5	5.39
60	14	7.45
80	18	11.44
100	22	19.77

particles have great influence on antibacterial performance. Furthermore, reactive oxygen species (ROS) molecules react with the cytoplasmic membrane, peptidoglycan layer, DNA, lipids, proteins, and other physiological processes when they are produced. The reaction between positively charged nickel molecules and negatively charged microbial cell membrane causes protein and other intercellular constituents to flow out, eventually destroying the cell [43]. By increasing the concentration, the zone of inhibition increases and the prepared NPs shown highest activity than earlier reports as shown in Table 1.

Prepared NPs were compared with Metformin HCl (Standard) to investigate the antidiabetic potential based on α-amylase inhibitory effectiveness (Fig. 9). The α-amylase inhibitory effectiveness of prepared NPs was compared based on their resulting IC_{50} values. Moreover, hyperglycemia is treated with certain phytopharmaceuticals of medicinal importance to regulate diabetes. The therapy improves glucose consumption by the body cells or by decreasing the absorption of the carbohydrates eventually by the inhibition of the α-amylase enzyme. During the experiment, standard metformin showed inhibitory effects on the α-amylase activity with an IC_{50} value of 307.14 μg mL^{-1}. However, the prepared NiO NPs from *A.bilimbi* fruit exhibited α-amylase inhibitory activity with an IC_{50} value of 311.26 μg mL^{-1} Compared to NiO NPs prepared using *Areca catechu* [44], IC_{50} obtained from the present work is greater. Even though % of inhibition is lesser at 20 and 40 μg/ml, it increases gradually and good results are achieved for 100 μg/ml as given in Table 2 [28]. As a result, NPS showed dose-dependent antidiabetic activity as compared to Metformin ($p < 0.005$). It was concluded from our *In vitro* experiments that, NPs constrain good α-amylase activity.

The cytotoxic evaluation of biosynthesized NiO NPs against HCT116 cell-line cancer cells and L929 fibroblast was carried out using an MTT assay and shown in Fig. 10. The size of the produced nanoparticles, their shape, and the surface to volume ratio all significantly influence the cytotoxicity of the material [45]. Possibly, the metal oxide NP's entered inside the cell and may induce intracellular oxidative stress by exasperating the steadiness between oxidants and antioxidants [46]. Secondly, the reactive oxygen species formed on the surface of NPs in the presence of light may exacerbate oxidative stress to the microbial cell, leading to cell death. After treating the HCT116 cell line with eco-friendly biosynthesized NiO NPs, dead cells appeared with a change in morphology. Eventually, the generated NPs can infiltrate into the cell membrane and destroy microbes [30]. About cell death, a minimum

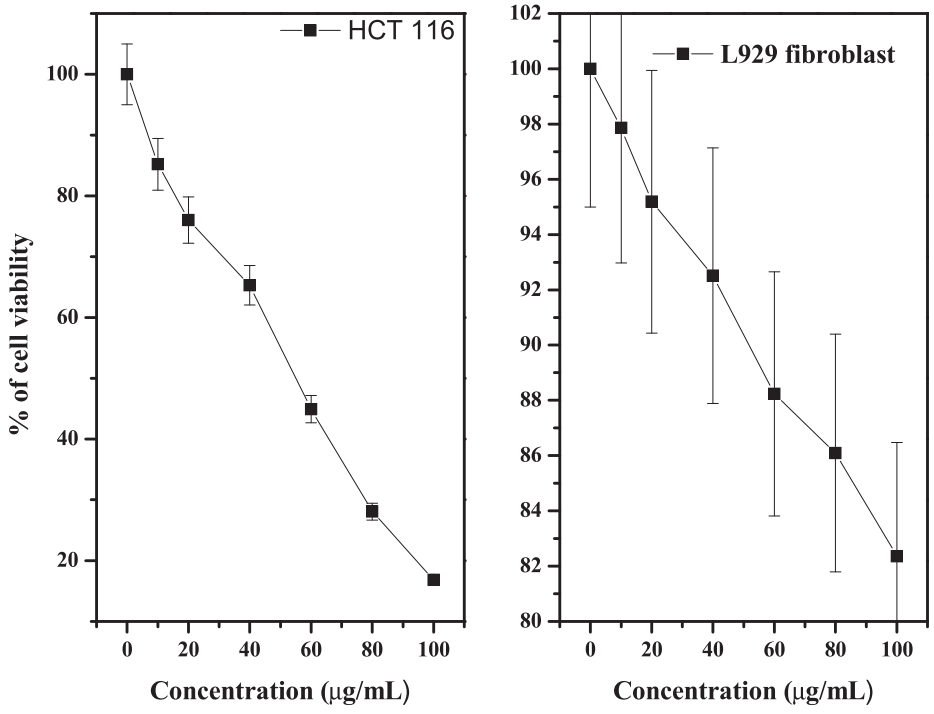

Fig. 10. Cell Viability of NiO NPs against HCT116 and L929 (10–100 μg/ml).

Table 3
Cytotoxicity of NPs against HCT 119 *and L929.*

Concentration (µg/mL)	Cell viability (%)	
	HCT 119 cancer cell	L929 fibroblast
Control	100 ± 5	100 ± 5
10	85.204 ± 4.260	97.860 ± 4.893
20	76.020 ± 3.801	95.187 ± 4.759
40	65.306 ± 3.265	92.513 ± 4.625
60	44.897 ± 2.244	88.235 ± 4.411
80	28.061 ± 1.403	86.096 ± 4.304
100	16.836 ± 0.841	82.352 ± 4.117

concentration for optimized NPs is sufficiently well to induce it. Interestingly, the microorganism carries a negative charge; however, the metal oxide possesses a positive charge, ultimately which causes an electromagnetic attraction between them. After treatment with different concentrations (20–100 µg mL^{-1}), the plating efficiency of HCT116 cells declines, as proved by the reduction in the number of cancer cells formed. The minimum inhibition was observed at 20 µgmL^{-1} and maximum at 100 µg mL^{-1} respectively, compared to regular cisplatin taken as 100 % and the cell viability % was given in Table 3 for HCT 116 and L929. The cell population was decreased in HCT116 cancer cells with IC_{50} density was found to be 55 µgmL^{-1}. It's obvious that more Ni^{2+} ions interact with the cell membrane, the higher injury is caused to the cancer cell membrane, and however, a comprehensive understanding of the biochemical mechanism in this *A. bilimbi* mediated NiO nanoparticles biosynthesis is a prerequisite and also similar to the report obtained by Niloufar Abbaszadeh et al., [47], Maryam Hosseinkhah et al., [48] against breast cancer cells. Fig. 10 showed cytotoxic effects on a cell line from a human breast cancer. When compared to malignant cells, produced nanoparticles were less hazardous to healthy cells (fibroblast L929).

The anticancer mechanism of ROS (shown in Fig. 11) is primarily formed by the mitochondrial electron transport chain under oxidative stress. Free radicals can be converted to less toxic molecules via enzymes to reduce the damage caused by ROS. For example, superoxide dismutase (SOD) converts superoxide anion to hydrogen peroxide, and hydrogen peroxide can be turned to water using catalyze or glutathion peroxidase enzymes [49]. These reactions caused an imbalance between the biological systems of the cells, which quickly detoxify the reactive intermediates, and the formation of ROS, which in turn caused the cancer cells to be damaged. The comparative anticancer study of NiO NPs made with various plant extracts is provided in Table 4, which clarifies that NiO NPs made with *Averrhoa bilimbi* have better anticancer activity than earlier reports.

4. Conclusion

The results of the current study conclude that *A. bilimbi* has a potent antidiabetic and cytotoxic effect, which was further enhanced by the nano-incorporation of nickel oxide. The powder XRD patterns confirm the formation of high crystalline cubic structured fmm space group nickel oxide. The functional groups and metal–oxygen bond were identified by FTIR spectroscopy. The bandgap was calculated as 3.2eV using Tauc's equation and the absorption peak at 340 nm elucidates the formation of NiO nanoparticles. Spherical nanoparticles in the size range of 100–120 nm were confirmed by SEM analysis. The superparamagetism property of the NiO NPs were exhibited by the absence of magnetic saturation, coercivity and retentivity from M-H curve. The antibacterial property was tested against *E.coli* and *S.aureus* for three different concentrations (50 µg mL^{-1}, 100 µg mL^{-1}, and 150 µg mL^{-1}). *Averrhoa bilimbi* assisted nickel oxide nanoparticles exhibit potent antidiabetic activity on α-amylase inhibitory effectiveness with IC_{50} of 311.26 µg mL^{-1} ($p < 0.005$) and also with earlier reports. Finally, the cytotoxic effects of nickel oxide nanoparticles was studied in cultured human colorectal cancer cells (HCT-116), which exhibited significant anticancer activity with 55 µg mL^{-1} at 50 % inhibition concentration (IC_{50}). Due to the results obtained from the antibacterial, antidiabetic, and anticancer activities of biosynthesized NiO nanoparticles and their

Table 4
Anticancer properties of NiO NPs using different plant extracts.

Reducing agent	Type of cell	IC_{50}value	Ref. No.
Solanum trilobatum	A549	92	[9]
Areca catechu	A549	93.349	[44]
As-purchased	HTB-37	351.6	[50]
Chemical	A549	148	[51]
Curcuma longa	HepG2	129.44	[52]
Averrhoa bilimbi	HCT 116	55	Present work

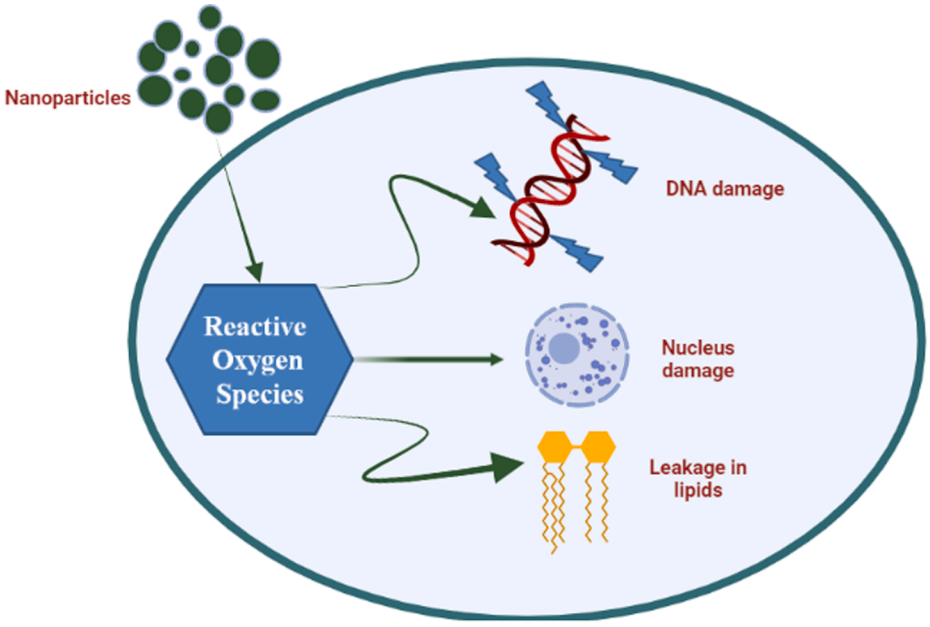

Fig. 11. A schematic image of NiO NPs with ROS.

proper physical and chemical properties, they might be suitable to pharmaceutical applications.

CRediT authorship contribution statement

V. Haritha: Methodology, Investigation, Writing – original draft. **S. Gowri:** Formal analysis, Investigation. **B. Janarthanan:** Conceptualization, Data curation. **Md. Faiyazuddin:** Resources. **C. Karthikeyan:** Formal analysis. **S. Sharmila:** Formal analysis, Conceptualization, Writing – review & editing, Project administration, Data curation.

Declaration of Competing Interest

The authors declare that they have no known competing financial interests or personal relationships that could have appeared to influence the work reported in this paper.

Data availability

The data that has been used is confidential.

References

[1] Y. Yao, Y. Zhou, L. Liu, Y. Xu, Q. Chen, Y. Wang, S. Wu, Y. Deng, J. Zhang, A. Shao, Nanoparticle-Based Drug Delivery in Cancer Therapy and Its Role in Overcoming Drug Resistance, Front. Mol. Biosci. 7 (2020), https://doi.org/10.3389/fmolb.2020.00193.

[2] N. Sisubalan, V.S. Ramkumar, A. Pugazhendhi, C. Karthikeyan, K. Indira, K. Gopinath, A.S.H. Hameed, M.H.G. Basha, ROS-mediated cytotoxic activity of ZnO and CeO_2 nanoparticles synthesized using the Rubia cordifolia L. leaf extract on MG-63 human osteosarcoma cell lines, Environ. Sci. Pollut. Res. 25 (11) (2018) 10482–10492, https://doi.org/10.1007/s11356-017-0003-5.

[3] S. Iravani, Green synthesis of metal nanoparticles using plants, Green Chem. 13 (10) (2011) 2638, https://doi.org/10.1039/c1gc15386b.

[4] D. Zhang, X.-L. Ma, G.u. Yan, H.e. Huang, G.-W. Zhang, Green Synthesis of Metallic Nanoparticles and Their Potential Applications to Treat Cancer, Front. Chem. 8 (2020) 799, https://doi.org/10.3389/fchem.2020.00799.

[5] A. Sophia, M.d. Faiyazuddin, P. Alam, M.T. Hussain, F. Shakeel, GC–MS characterization and evaluation of antimicrobial, anticancer and wound healing efficiency of combined ethanolic extract of *Tridax procumbens* and *Acalypha indica*, J. Mol. Struct. 1250 (2022) 131678, https://doi.org/10.1016/j.molstruc.2021.131678.

[6] R.S. Rimal Isaac, G. Sakthivel, C.h. Murthy, Green Synthesis of Gold and Silver Nanoparticles Using *Averrhoa bilimbi* Fruit Extract, J. Nanotech. (2013) 906592, https://doi.org/10.1155/2013/906592.

[7] M.S. Nair, K. Soren, V. Singh, B. Boro, Anticancer Activity of Fruit and Leaf Extracts of *Averrhoa bilimbi* on MCF-7 Human Breast Cancer Cell Lines: A Preliminary Study, Austin. J. Pharmacol. Ther. 4 (2) (2016) 1082.

[8] S.B. Kurup, S. Mini, *Averrhoa bilimbi* fruits attenuate hyperglycemia-mediated oxidative stress in streptozotocin-induced diabetic rats, J. Food Drug Anal. 25 (2) (2017) 360–368, https://doi.org/10.1016/j.jfda.2016.06.007.

[9] M. Bonomo, Synthesis and characterization of NiO nanostructures: a review, J. Nanopart. Res. 20 (2018) 222, https://doi.org/10.1007/s11051-018-4327-y.

[10] P. Vijaya Kumar, A. Jafar Ahamed, M. Karthikeyan, Synthesis and characterization of NiO nanoparticles by chemical as well as green routes and their comparisons with respect to cytotoxic effect and toxicity studies in microbial and MCF7 cancer cell models, SN Appl. Sci. 1 (2019) 1083, https://doi.org/10.1007/s42452-019-1113-0.

[11] M. Karthikeyan, A. Jafar Ahamed, C. Karthikeyan, P. Vijaya Kumar, Enhancement of antibacterial and anticancer properties of pure and REM doped ZnO nanoparticles synthesized using *Gymnema sylvestre* leaves extract, SN Appl. Sci. 1 (2019) 355, https://doi.org/10.1007/s42452-019-0375-x.

[12] Z. Sabouri, A. Akbari, H.A. Hosseini, M. Khatami, M. Darroudi, Green-based biosynthesis of nickel oxide nanoparticles in Arabic gum and examination of their cytotoxicity, photocatalytic and antibacterial effects, Green Chem. Lett. Rev. 14 (2) (2021) 404–414, https://doi.org/10.1080/17518253.2021.1923824.

[13] R. Lefojane, P. Direko, P. Mfengwana, S. Mashele, N. Matinise, M. Maaza, M. Sekhoacha, Green Synthesis of Nickel Oxide (NiO) Nanoparticles Using *Spirostachys Africana* Bark Extract, Asian J. Sci. Res. 13 (4) (2020) 284–291, https://doi.org/10.3923/ajsr.2020.284.291.

[14] S. Uddin, L.B. Safdar, S. Anwar, J. Iqbal, S. Laila, B.A. Abbasi, M.S. Saif, M. Ali, A. Rehman, A. Basit, Y. Wang, U.M. Quraishi, Green Synthesis of Nickel Oxide Nanoparticles from Berberis balochistanica Stem for Investigating Bioactivities, Molecules 26 (6) (2021) 1548, https://doi.org/10.3390/molecules26061548.

[15] A.A. Ezhilarasi, J.J. Vijaya, K. Kaviyarasu, X.u. Zhang, L.J. Kennedy, Green synthesis of nickel oxide nanoparticles using Solanum trilobatum extract for cytotoxicity, antibacterial and photocatalytic studies, Surf. Interfaces 20 (2020) 100553, https://doi.org/10.1016/j.surfin.2020.100553.

[16] J. Iqbal, B.A. Abbasi, R. Ahmad, M. Mahmoodi, A. Munir, S.A. Zahra, A. Shahbaz, M. Shaukat, S. Kanwal, S. Uddin, T. Mahmood, R. Capasso, Phytogenic Synthesis of Nickel Oxide Nanoparticles (NiO) Using Fresh Leaves Extract of *Rhamnus triquetra* (Wall.) and Investigation of Its Multiple In Vitro Biological Potentials, Biomedicines 8 (5) (2020) 117, https://doi.org/10.3390/biomedicines8050117.

[17] A.A. Ezhilarasi, J.J. Vijaya, L.J. Kennedy, K. Kaviyarasu, Green mediated NiO nano-rods using *Phoenix dactylifera* (Dates) extract for biomedical and environmental applications, Mater. Chem. Phys. 241 (2020) 122419, https://doi.org/10.1016/j.matchemphys.2019.122419.

[18] A. Haider, M. Ijaz, S. Ali, J. Haider, M. Imran, H. Majeed, I. Shahzadi, M.M. Ali, J. A. Khan, M. Ikram, Green Synthesized Phytochemically (Zingiber officinale and Allium sativum) Reduced Nickel Oxide Nanoparticles Confirmed Bactericidal and Catalytic Potential, Nanoscale Res. Lett. 15 (1) (2020), https://doi.org/10.1186/s11671-020-3283-5.

[19] V. Helan, J.J. Prince, N.A. Al-Dhabi, M.V. Arasu, A. Ayeshamariam, G. Madhumitha, S.M. Roopan, M. Jayachandran, Neem leaves mediated preparation of NiO nanoparticles and its magnetization, coercivity and antibacterial analysis, Results Phys. 6 (2016) 712–718, https://doi.org/10.1016/j.rinp.2016.10.005.

[20] P. Kganyago, L.M. Mahlaule-Glory, M.M. Mathipa, B. Ntsendwana, N. Mketo, Z. Mbita, N.C. Hintsho-Mbita, Synthesis of NiO nanoparticles via a green route using Monsonia burkeana: The physical and biological properties, J. Photochem. Photobiol. B: Biol. 182 (2018) 18–26, https://doi.org/10.1016/j.jphotobiol.2018.03.016.

[21] A. Angel Ezhilarasi, J. Judith Vijaya, K. Kaviyarasu, L. John Kennedy, R. J. Ramalingam, H.A. Al-Lohedan, Green synthesis of NiO nanoparticles using Aegle marmelos leaf extract for the evaluation of in-vitro cytotoxicity, antibacterial and photocatalytic properties, J. Photochem. Photobiol. B: Biol. 180 (2018) 39–50, https://doi.org/10.1016/j.jphotobiol.2018.01.023.

[22] M.A. Rafique, S. Kiran, S. Javed, I. Ahmad, S. Yousaf, N. Iqbal, G. Afzalf, F. Rani, Green synthesis of nickel oxide nanoparticles using Allium cepa peels for degradation of Congo red direct dye: an environmental remedial approach, Water Sci. Technol. 84 (10–11) (2021) 2793, https://doi.org/10.2166/wst.2021.237.

[23] T. Adinaveen, T. Thenmozhi Karnan, S.A.S. Selvakumar, Photocatalytic and optical properties of NiO added Nephelium lappaceum L. peel extract: An attempt to convert waste to a valuable product, Heliyon 5 (2019), e01751, https://doi.org/10.1016/j.heliyon.2019.e01751.

[24] J. Iqbal, B.A. Abbasi, T. Mahmood, S. Hameed, A. Munir, S. Kanwal, Green synthesis and characterizations of Nickel oxide nanoparticles using leaf extract of *Rhamnus virgata* and their potential biological applications, Appl. Organomet. Chem. 33 (8) (2019), https://doi.org/10.1002/aoc.v33.810.1002/aoc.4950.

[25] Z. Sabouri, N. Fereydouni, A. Akbari, H.A. Hosseini, A. Hashemzadeh, M.S. Amiri, R. Kazemi Oskuee, M. Darroudi, Plant-based synthesis of NiO nanoparticles using salvia macrosiphon Boiss extract and examination of their water treatment, Rare Met. 39 (10) (2020) 1134–1144, https://doi.org/10.1007/s12598-019-01333-z.

[26] A.A. Ezhilarasi, J.J. Vijaya, K. Kaviyarasu, M. Maaza, A. Ayeshamariam, L. J. Kennedy, Green synthesis of NiO nanoparticles using *Moringa oleifera* extract and their biomedical applications: Cytotoxicity effect of nanoparticles against HT-29 cancer cells, J. Photochem. Photobiol. B: Biol. 164 (2016) 352–360, https://doi.org/10.1016/j.jphotobiol.2016.10.003.

[27] M.A. Nasseri, F. Ahrari, B. Zakerinasab, A green biosynthesis of NiO nanoparticles using aqueous extract of Tamarix serotina and their characterization and application, Appl. Organomet. Chem. 30 (12) (2016) 978–984, https://doi.org/10.1002/aoc.3530.

[28] A. Ayesha Mariam, M. Kashif, S. Arokiyaraj, M. Bououdina, M.G. V. Sankaracharyulu, M. Jayachandran, U. Hashim, Bio-Synthesis of NiO and Ni Nanoparticles And Their Characterization, Dig. J. Nanomater. Bios. 9 (3) (2014) 1007.

[29] Miessya Wardani, Yoki Yulizar, Iman Abdullah, Dewangga Oky Bagus, Apriandanu, Synthesis of NiO nanoparticles via green route using Ageratum conyzoides L. leaf extract and their catalytic activity, IOP Conf. Series Mater. Sci. Eng. 509 (2019) 012077, https://doi.org/10.1088/1757-899X/509/1/012077.

[30] R.G. Saratale, H.S. Shin, G. Kumar, G. Benelli, D.-S. Kim, G.D. Saratale, Exploiting antidiabetic activity of silver nanoparticles synthesized using Punicagranatum leaves and anticancer potential against human liver cancer cells (HepG2), Artificial Cells. Nanomed. Biotechnol. 46 (2018) 211, https://doi.org/10.1080/21691401.2017.1337031.

[31] S. Sagadevan, S. Vennila, P. Singh, J.A. Lett, M.R. Johan, A.R. Marlinda, B. Muthiah, M. Lakshmipathy, Facile synthesis of silver nanoparticles using *Averrhoa bilimbi* L and Plum extracts and investigation on the synergistic bioactivity using in vitro models, Green Process. Synth, 8 (1) (2019) 873–884, https://doi.org/10.1515/gps-2019-0058.

[32] M.N. Siddique, A. Ahmed, P. Tripathi, Electric transport and enhanced dielectric permittivity in pure and Al doped NiO nanostructures, J. Alloy. Compd. 735 (2018) 516–529, https://doi.org/10.1016/j.jallcom.2017.11.114.

[33] P. Archana, B. Janarthanan, S. Bhuvana, P. Rajiv, S. Sharmila, Concert of zinc oxide nanoparticles synthesized using *Cucumis melo* by green synthesis and the antibacterial activity on pathogenic bacteria, Inorg. Chem. Commun. 137 (2022) (2022), 109255, https://doi.org/10.1016/j.inoche.2022.109255.

[34] K. Lingaraju, H. Raja Naika, H. Nagabhushana, K. Jayanna, S. Devaraja, G. Nagaraju, Biosynthesis of Nickel oxide Nanoparticles from Euphorbia heterophylla (L.) and their biological Application, Arab. J. Chem. 13 (3) (2020) 4712, https://doi.org/10.1016/j.arabjc.2019.11.003.

[35] R. Ramalingam, M.H.U.T. Fazil, N.K. Verma, K.D. Arunachalam, Green synthesis, characterization and antibacterial valuation of electrospun nickel oxide nanofibers, Mater. Lett. 256 (2019), 126616, https://doi.org/10.1016/j.matlet.2019.126616.

[36] Z. Sabouri, A. Akbari, H.A. Hosseini, A. Hashemzadeh, M. Darroudi, Eco-Friendly Biosynthesis of Nickel Oxide Nanoparticles Mediated by Okra Plant Extract and Investigation of Their Photocatalytic, Magnetic, Cytotoxicity, and Antibacterial Properties, J. Clust. Sci. 30 (6) (2019) 1425–1434, https://doi.org/10.1007/s10876-019-01584-x.
[37] M. Abdur Rahman, R. Radhakrishnan, Microstructural properties and antibacterial activity of Ce doped NiO through chemical method, SN Appl. Sci. 1 (2019) 221, https://doi.org/10.1007/s42452-019-0232-y.
[38] A. Gandhi, S. Wu, Strong Deep-Level-Emission Photoluminescence in NiO Nanoparticles, Nanomaterials 7 (8) (2017) 231, https://doi.org/10.3390/nano7080231.
[39] Abdul rahman Syed ahamed Haja Hameed, Chandrasekaran Karthikeyan, Abdulazees Parveez Ahamed, Nooruddin Thajuddin et al, In vitro antibacterial activity of ZnO and Nd doped ZnO nanoparticles against ESBL producing Escherichia coli and Klebsiella pneumonia, Sci. Rep. 6 (2016) 24312.
[40] K. Sudalai Muthu, P. Perumal, Synthesis and characterization of NiO Nanoparticles using egg white method, J. Mater. Sci.: Mater. Electron. 28 (2017) 9612.
[41] K. Karthik, G.K. Selvan, M. Kanagaraj, S. Arumugam, N.V. Jaya, Particle size effect on the magnetic properties of NiO nanoparticles prepared by a precipitation method, J. Alloy. Compd. 509 (1) (2011) 181–184, https://doi.org/10.1016/j.jallcom.2010.09.033.
[42] J.B. Yi, J. Ding, Y.P. Feng, G.W. Peng, G.M. Chow, Y. Kawazoe, B.H. Liu, J.H. Yin, S. Thongmee, Size-dependent magnetism and spin-glass behavior of amorphous NiO bulk, clusters, and nanocrystals: Experiments and first-principles calculations, Phys Rev. B 76 (22) (2007), https://doi.org/10.1103/PhysRevB.76.224402.
[43] N. Pourmehdi, Z. Moradi-Shoeili, A.S. Naeemi, A. Salehzadeh, Biosynthesis of NiFe2O4@Ag nanocomposite and assessment of its effect on expression of norA gene in Staphylococcus aureus, Chem. Biodivers. 17 (6) (2020), e2000072, https://doi.org/10.1002/cbdv.202000072.
[44] S. U r, R.K. C r, K.M. M s, V.S. Betageri, L. M s, R. Veerapur, G. Lamraoui, A.A. Al-Kheraif, A.M. Elgorban, A. Syed, C. Shivamallu, S.P. Kollur, Biogenic Synthesis of NiO Nanoparticles Using Areca catechu Leaf Extract and Their Antidiabetic and Cytotoxic Effects, Molecules 26 (9) (2021) 2448, https://doi.org/10.3390/molecules26092448.
[45] C. Karthikeyan, N. Sisubalan, M. Sridevi, K. Varaprasad, M.H. Ghouse Basha, W. Shucai, R. Sadiku, Biocidal chitosan-magnesium oxide nanoparticles *via* a green precipitation process, J. Hazard. Mater. 411 (2021) 124884, https://doi.org/10.1016/j.jhazmat.2020.124884.
[46] S. Singh Vandana, Shashikant C. Dhawale, Faiyaz Shakeel, Md Faiyazuddin, Sultan Alshehri, *Antiarthritic Potential of Calotropi sprocera* leaf fractions in FCA-induced arthritic rats: Involvement of cellular inflammatory mediators and other biomarkers. Agriculture 11(1) (2021) 68.
[47] N. Abbaszadeh, N. Jaahbin, A. Pouraei, F. Mehraban, M. Hedayati, A. Majlesi, F. Akbari, S.A.S. Shandiz, A. Salehzadeh, Preparation of Novel Nickel Oxide@Glutamic/Thiosemicarbazide Nanoparticles: Implications for Cytotoxic and Anti-cancer Studies in MCF-7 Breast Cancer Cells, J. Clust. Sci. 10 (5) (2021) 230, https://doi.org/10.1007/s10876-021-01995-9.
[48] M. Hosseinkhah, R. Ghasemian, F. Shokrollahi, S.R. Mojdehi, M.J.S. Noveiri, M. Hedayati, M. Rezaei, A. Salehzadeh, Cytotoxic Potential of Nickel Oxide Nanoparticles Functionalized with Glutamic Acid and Conjugated with Thiosemicarbazide (NiO@Glu/TSC) Against Human Gastric Cancer Cells, J. Clust. Sci. 33 (5) (2022) 2045–2053, https://doi.org/10.1007/s10876-021-02124-2.
[49] K. Mohamed, K. Zine, K. Fahima, E. Abdelfattah, S.M. Sharifudin, K. Duduku, NiO nanoparticles induce cytotoxicity mediated through ROS generation and impairing the antioxidant defense in the human lung epithelial cells (A549): Preventive effect of *Pistacia lentiscus* essential oil, Toxicol. Rep. 5 (2018) 480–488, https://doi.org/10.1016/j.toxrep.2018.03.012.
[50] M. Abudayyak, E. Güzel, G. Özhan, Cytotoxic, Genotoxic, and Apoptotic Effects of Nickel Oxide Nanoparticles in Intestinal Epithelial Cells, Turk. J. Pharm. Sci. 17 (4) (2020) 446–451, https://doi.org/10.4274/tjps.galenos.2019.76376.
[51] T. Kawakami, A. Miyajima, K. Komoriya, R. Kato, K. Isama, Effect of secondary particle size of nickel oxide nanoparticles on cytotoxicity in A549 cells, J. Toxicol. Sci. 47 (4) (2022) 151–157, https://doi.org/10.2131/jts.47.151.
[52] S. Faisal, N.S. Al-Radadi, H. Jan, Abdullah, S.A. Shah, S. Shah, M. Rizwan, Z. Afsheen, Z. Hussain, M.N. Uddin, M. Idrees, N. Bibi, Curcuma longa Mediated Synthesis of Copper Oxide, Nickel Oxide and Cu-Ni Bimetallic Hybrid Nanoparticles: Characterization and Evaluation for Antimicrobial, Anti-Parasitic and Cytotoxic Potentials, Coatings 11 (7) (2021) 849, https://doi.org/10.3390/coatings11070849.